

Electronic Supplementary Information

Carbon-coated TiNb₂O₇ nanosheet arrays as self-supported high mass-loading anode for flexible Li-ion battery†

Jinquan Zhou,^a Haoyang Dong,^a Yao Chen,^a Yihua Ye,^a Liang Xiao,^a Bohua Deng^{*a} and Jinping Liu^{*ab}

^a School of Chemistry, Chemical Engineering and Life Science, Wuhan University of Technology, Wuhan, 430070, Hubei, China. E-mail: dengbh@whut.edu.cn

^b State Key Laboratory of Advanced Technology for Materials Synthesis and Processing, Wuhan University of Technology, Wuhan, 430070, Hubei, China. E-mail: liujp@whut.edu.cn

Experimental section

Synthesis of carbon-coated TNO NSAs

The carbon-coated TNO NSAs directly grown on the carbon cloth were prepared by a facile solvothermal process and subsequent carbon-coating treatment. First, a piece of carefully cleaned carbon cloth (2.5 cm × 2.5 cm, WOS1009, Cetech Co. Ltd., Taiwan) was placed in a Teflon-lined reactor (100 mL, sealed by a stainless-steel autoclave) containing a solution of niobium chloride (NbCl₅, 1.8 mmol), tetrabutyl titanate (Ti(OC₄O₉)₄, 0.9 mmol) and ca. 0.7 g HF in 50 mL glycol. The reactor was heated to and held at 200 °C for 20 h. After cooling down, the modified carbon cloth (denoted as precursor) was picked up, and then cleaned with ethanol and distilled water successively for several times. Secondly, the precursor was coated with polydopamine by immersing it in a solution containing 50 mg dopamine hydrochloride in a Tris buffer (75 mL, 10 mol L⁻¹; pH=8.5) for 20 h under continuous stirring. Then, the polydopamine-coated precursor was annealed at 750 °C for 5 h in Ar atmosphere to obtain the carbon-coated TNO NSAs. The average mass loading of TNO materials on the carbon cloth was estimated by the average mass difference between the reference carbon cloth and modified carbon cloth with TNO NSAs (of the same area or size). The reference carbon cloth was prepared by a control experiment which is similar to that for

the pristine TNO NSAs, but NbCl_5 and $\text{Ti}(\text{OC}_4\text{O}_9)_4$ were not added in the solution for hydrothermal reaction (therefore no TNO materials present on the carbon cloth). The coating-carbon content on the carbon-coated TNO NSAs was subtracted based on the TGA analysis. The mass loading varies between 3.0 and 10.0 mg cm^{-2} and depends on the experimental conditions (solvothermal time and etc.).

Physical characterizations

The surface morphology of as-prepared materials was examined by field emission scanning electron microscopy (FE-SEM, Hitachi S-4800, Japan), and the transmission electron microscopy (TEM) were characterized with JEM-2010FEF (200 kV). The powder X-ray diffraction (XRD) was performed with Bruker D-8 Advance (Cu $K\alpha$). The surface chemical states of the materials were analyzed with X-ray photoelectron spectroscopy (XPS, Escalab 250-Xi, USA). The electronic conductivity of the pristine and carbon-coated TNO NSAs were measured by the four-point probe method with Keithley 6517B. The TGA and BET data of the carbon-coated TNO NSAs were obtained with Mettler Toledo TGA/DSC and V-Sorb 2800TP, respectively.

Electrochemical characterizations

The galvanostatic charge/discharge performances were examined by LAND CT2001A battery testing system (Wuhan Jinnuo, China), and the measured cycling performances are in statistic error of $\pm 5\%$. Cyclic voltammetry (CV) was performed with CHI-660 electrochemical workstation (Shanghai Chenhua). Electrochemical impedance characterization was carried out on a PGSTAT100N electrochemical workstation (Autolab), at open circuit potential (OCV) in the frequency range from 0.005 Hz to 1000 kHz and with a potential amplitude of 10 mV applied during testing. The CR2032-type coin or soft package cells were assembled in an Ar-filled glove box for half-cell or full battery testing. In the half cells, Li foil was used as the counter electrode, the electrodes of modified carbon cloths with directly grown TNO materials or LNMO were used as the working electrode. In the full batteries, the carbon-coated TNO NSAs and the LNMO electrodes were applied as the anode and cathode, respectively. The LNMO cathodes were prepared by slurry-coating with a doctor blade (on Al foil for

coin cells and on carbon cloth for soft-packaged battery, respectively). The slurry was prepared by homogeneously mixing the LNMO powders, acetylene black and fluoride (PVDF) in a weight ratio of 8:1:1 in N-methylpyrrolidone (NMP). All the electrodes were vacuum-dried at 130 °C for 5 h before cell preparation. The electrolyte of 1 M LiPF₆ in ethylene carbonate (EC) and dimethyl carbonate (DMC) (1:1 in volume) were commercially supplied by Guotai Huarong (China) and directly used. The mass-loading of the TNO NSAs at the anode and LNMO at the cathode for the full battery is about 5.8 and 14.5 mg cm⁻², respectively. The model flexible batteries in soft packages were hot-sealed in a PE polymer bag of ca. 6.25 cm² (2.5 cm × 2.5 cm). The gravimetric energy/power densities of the full batteries (*E* and *P*) are calculated with $E = \int_{t_1}^{t_2} IV(t)dt$ and $P = E / \Delta t$, where *I* is the constant current density (A g⁻¹ or A cm⁻³), *V*(*t*) is the working voltage at *t*, *dt* is time differential, *t*₁ and *t*₂ (s) are the start and end time of discharging, and Δt is the total discharging time. The mass used for calculation is based on the active anode and cathode materials.

Table S1 The representative nanoarray materials in previously reported research.

Sample	Typical characteristics	Mass Loading (mg cm ⁻²)	Ref.
CNTs//Li ₄ Ti ₅ O ₁₂	nanowire	2.34	1
ZnCo ₂ O ₄	nanowire	0.3-0.6	2
Li ₄ Ti ₅ O ₁₂ -C	nanotube	0.42	3
MnCo ₂ O ₄	nanosheet	3	4
CoMoO ₄	nanowire	2.0-2.2	5
NiCo ₂ S ₄	nanotube	1.2	6
CoFe ₂ O ₄	nanowire	1.7-2.0	7
Zn ₃ P ₂	nanowire	3	8
Fe ₃ O ₄	nanotube	0.8-1.2	9
Mo-doped SnS ₂	nanosheet	0.8	10
V ₂ O ₅	nanosheet	2.1	11
Co ₄ N	nanoarray	2.1-2.5	12
Carbon coated MoS ₂	nanosheet	0.45	13
Co ₃ O ₄	nanosheet	0.53	14
Li ₄ Ti ₅ O ₁₂	cuboid	2.87	15
NiSe ₂	nanosheet	1.5-1.8	16
TiO ₂ @TiN	nanowire	1.5	17
TiO ₂ @rutile SnO ₂	nanorod	1.2	18

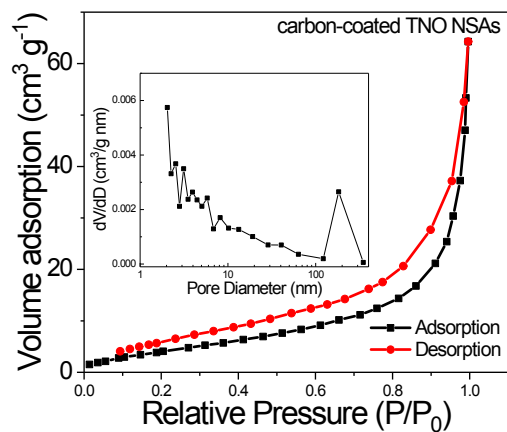


Fig. S1 Nitrogen adsorption/desorption isotherm and pore size distribution of the carbon-coated TNO NSAs.

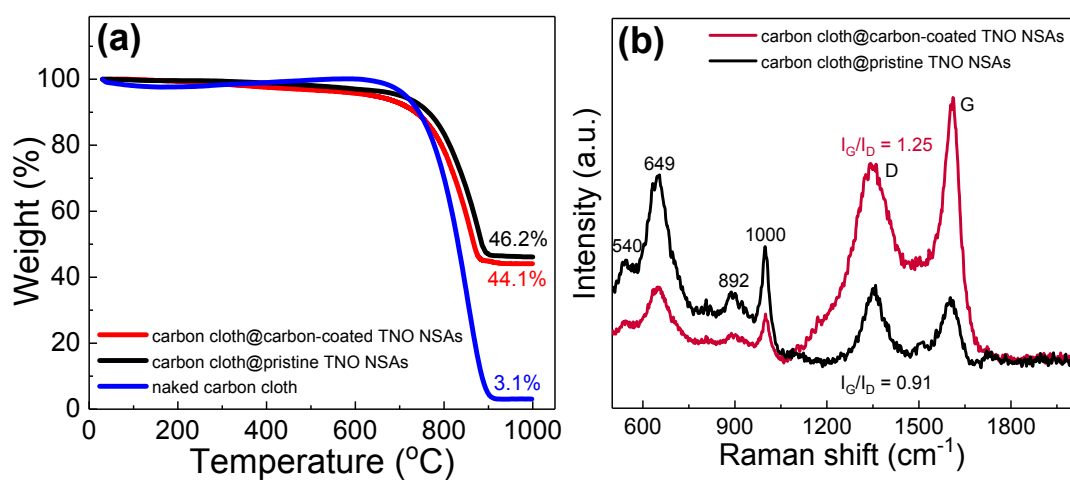


Fig. S2 (a) TGA analysis. (b) Raman spectra.

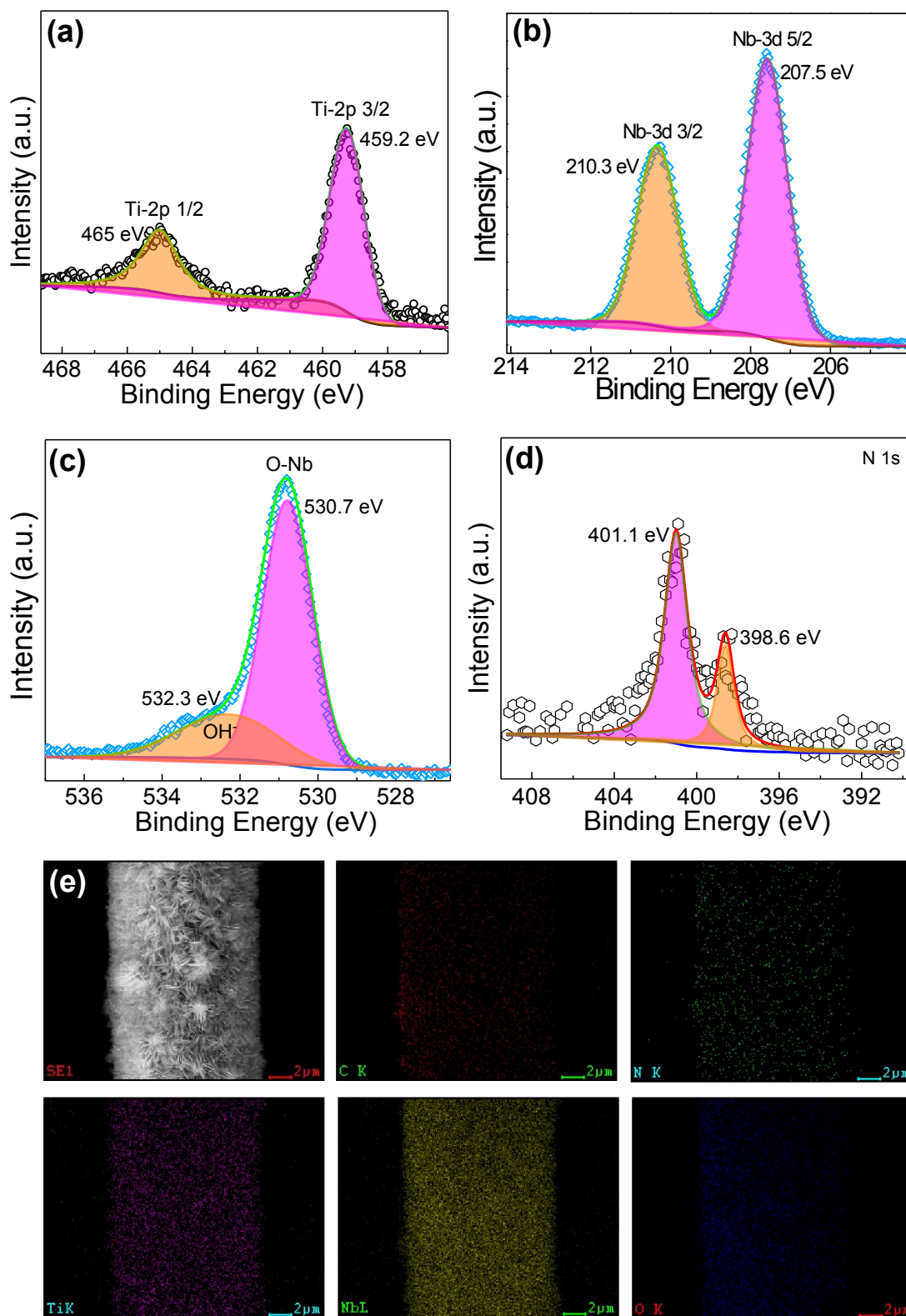


Fig. S3 (a-d) Ti 2p, Nb 3d, O 1s and N 1s XPS absorption of the carbon-coated TNO NSAs. (e) The elemental mapping images.

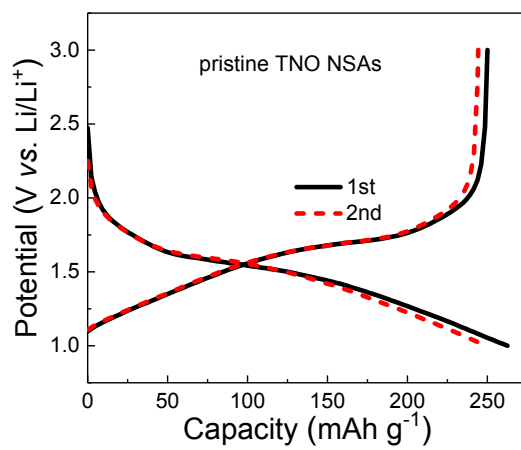


Fig. S4 Discharge/charge profiles of the pristine TNO NSAs in the initial two cycles at 1 C.

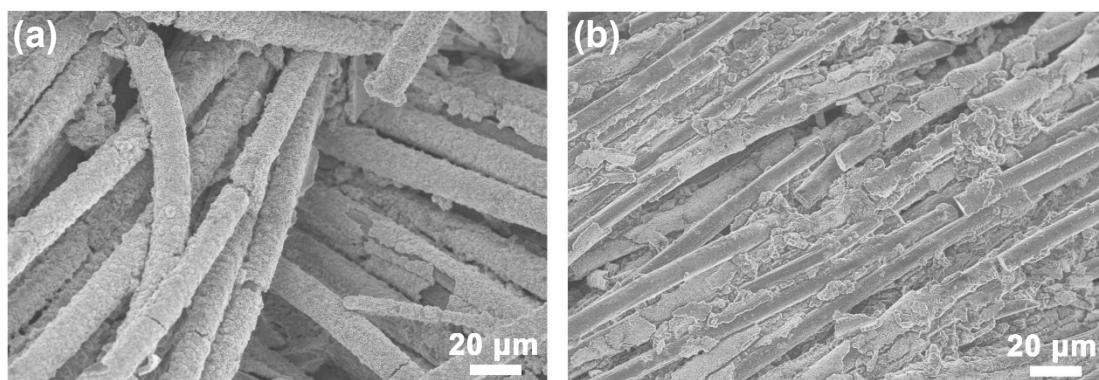


Fig. S5 The overall SEM images: (a) the carbon-coated TNO NSAs after 2000 cycles; (b) the pristine TNO NSAs after 1000 cycles.

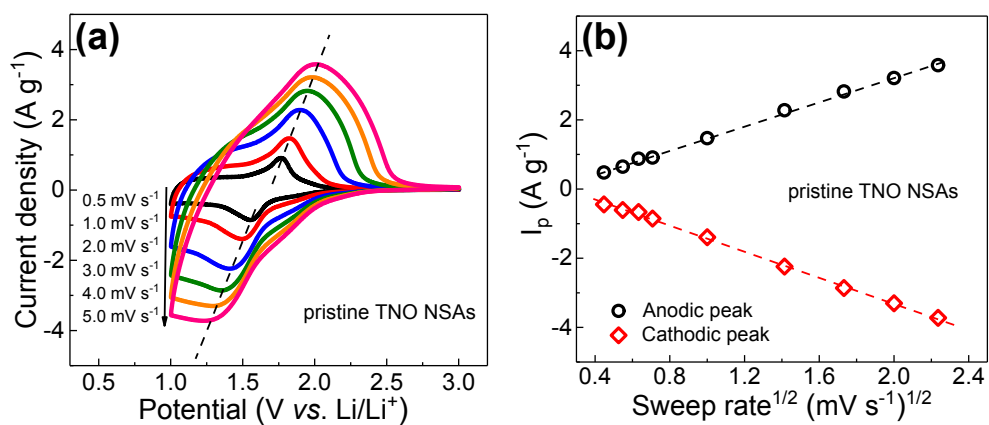


Fig. S6 (a) CV profiles of the pristine TNO NSAs at various sweep rates. (b) Plots of the peak current at ca. 1.70 V against sweep rates for the pristine TNO NSAs.

Table S2 The calculated diffusion coefficients of lithium ions (D_{Li^+}).

D_{Li^+} ($\text{cm}^2 \text{s}^{-1}$)	carbon coated TNO NSAs	pristine TNO NSAs
anodic peak	2.10×10^{-12}	1.55×10^{-12}
cathodic peak	2.06×10^{-12}	1.57×10^{-12}

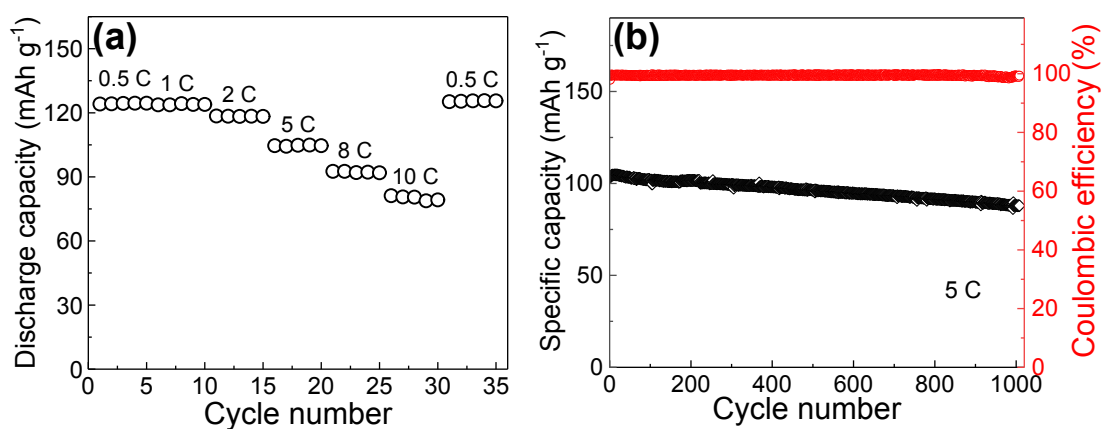


Fig. S7 LNMO: (a) Rate performance. (b) Cycling performance.

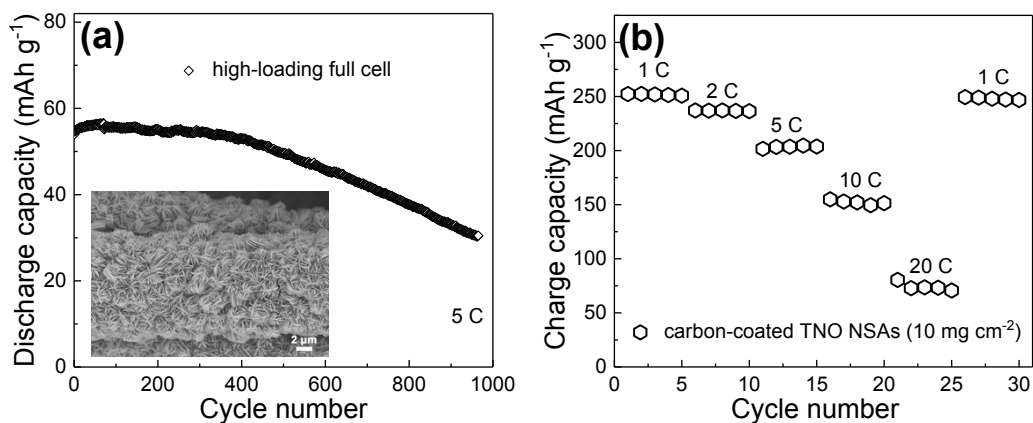


Fig. S8 (a) Cyclic performance of the high-loading full cell at 5 C (inset image: the high-loading carbon cloth). (b) Rate performances.

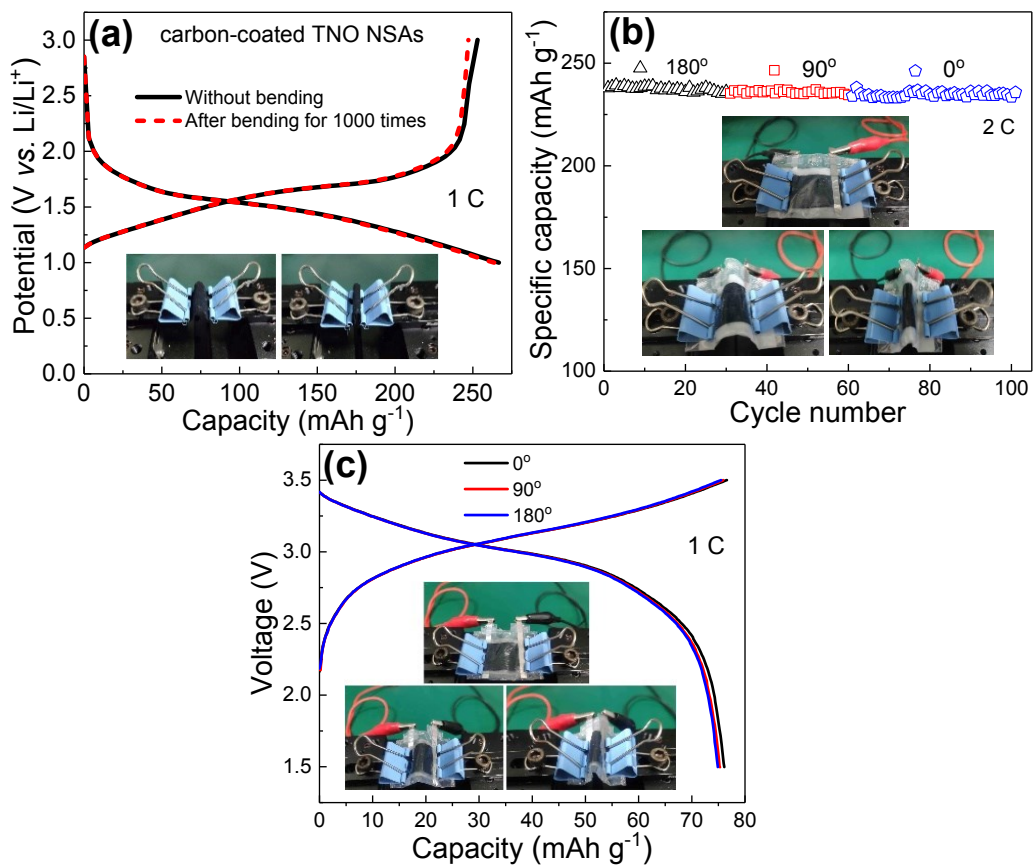


Fig. S9 (a) Charge/discharge profiles for the carbon-coated TNO NSAs with or without continuous bending (Inset images for continuous bending). (b) Cycling performance of the carbon-coated TNO NSAs under different bending angles. (c) Charge/discharge profiles of the full battery under different bending angles.

References:

- 1 W. Zuo, C. Wang, Y. Li, J. Liu, *Sci. Rep.* 2015, **5**, 7780.
- 2 B. Liu, J. Zhang, X. Wang, G. Chen, D. Chen, C. Zhou, G. Shen, *Nano Lett.* 2012, **12**, 3005–3011.
- 3 J. Liu, K. Song, P. A. van Aken, J. Maier, Y. Yu, *Nano Lett.* 2014, **14**, 2597–2603.
- 4 X. Hou, X. Wang, B. Liu, Q. Wang, T. Luo, D. Chen and G. Shen, *Nanoscale*, 2014, **6**, 8858–8864.
- 5 Y. Chen, B. Liu b, W. Jiang, Q. Liu, J. Liu, J. Wang, H. Zhang, X. Jing, *J. Power Sources*, 2015, **300**, 132–138.
- 6 X. Wu, S. Li, B. Wang, J. Liu, and M. Yu, *Phys. Chem. Chem. Phys.*, 2016, **18**, 4505–4512.
- 7 S. Zhao, J. Guo, F. Jiang, Q. Su, G. Du, *Mater. Res. Bull.*, 2016, **79**, 22–28.
- 8 W. Li, L. Gan, K. Guo, L. Ke, Y. Wei, H. Li, G. Shen and T. Zhai, *Nanoscale*, 2016, **8**, 8666–8672.
- 9 W. Qiu, M. Balogun, Y. Luo, K. Chen, Y. Zhu, X. Xiao, X. Lu, P. Liu, Y. Tong, *Electrochim. Acta*, 2016, **193**, 32–38.
- 10 Q. Chen, F. Lu, Y. Xia, H. Wang and X. Kuang, *J. Mater. Chem. A*, 2017, **5**, 4075–4083.
- 11 K. Ma, X. Liu, Q. Cheng, P. Saha, H. Jiang, C. Li, *J. Power Sources*, 2017, **357**, 71–76.
- 12 T. Wang, G. Chen, X. Liu, F. Chen, N. Zhang, J. Li, S. Liang, R. Ma, and G. Qiu, *ACS Appl. Energy Mater.*, 2018, **1**, 4432–4439.
- 13 N. Chen, C. Han, R. Shi, L. Xu, H. Li, Y. Liu, J. Li, B. Li, *Electrochim. Acta*, 2018, **283**, 36–44.
- 14 Q. Xie, R. Song, P. Zhao, Y. Zhang, S. Wu and D. Xie, *J. Mater. Chem. A*, 2018, **6**, 8388–8395.
- 15 C. Wang, X. Wang, C. Lin, and X. Zhao, *small*, 2019, **15**, 1902183.
- 16 X. Xiao, L. Ni, G. Chen, G. Ai, J. Li, T. Qiu, X. Liu, *J. Alloys Compd.*, 2020, **821**, 153218.
- 17 M. Balogun, C. Li, Y. Zeng, M. Yu, Q. Wu, M. Wu, X. Lu, Y. Tong, *J. Power Sources*, 2014, **272**, 946–953.
- 18 Q. Liu, L. Wang, K. Zhao, W. Yan, M. Liu, D. Wei, L. Xi, J. Zhang, *Electrochim. Acta*, 2020, **354**, 136727.